01 Oct 2005

Repeatable Nanostructures in Dielectrics by Femtosecond Laser Pulse Trains

Lan Jiang
Missouri University of Science and Technology, jianglan@mst.edu

Hai-Lung Tsai
Missouri University of Science and Technology, tsai@mst.edu

Recommended Citation

L. Jiang and H. Tsai, "Repeatable Nanostructures in Dielectrics by Femtosecond Laser Pulse Trains," *Applied Physics Letters*, American Institute of Physics (AIP), Oct 2005.
The definitive version is available at https://doi.org/10.1063/1.2093935

Repeatable nanostructures in dielectrics by femtosecond laser pulse trains

Lan Jiang and Hai-Lung Tsai[a)]
Laser-Based Manufacturing Laboratory, Department of Mechanical and Aerospace Engineering, University of Missouri-Rolla, Rolla, Missouri 65409

(Received 24 May 2005; accepted 20 August 2005; published online 3 October 2005)

Using the plasma model recent developed by the authors, this study predicts the existence of a constant ablation-depth zone with respect to fluence in femtosecond laser ablation of dielectrics, which has also been observed experimentally. It is found that the value of the constant ablation depth is significantly decreased by the pulse train technology. Repeatable nanostructures can be achieved with the parameters in the constant ablation-depth zone of a femtosecond pulse train, even when the laser system is subject to fluctuations in fluences. © *2005 American Institute of Physics*. [DOI: 10.1063/1.2093935]

Recent developments of optical devices make it possible to obtain almost any arbitrary pulse shapes. Many studies have been reported regarding pulse shaping and its effects on laser-materials interaction. For example, by using shaped pulse trains, (1) ionization process can be controlled;[1] (2) atoms can be selectively ionized;[2] (3) the ground-state rotational dynamics of molecules can be manipulated;[3] (4) chemical reactions can be controlled;[4] and (5) the x-ray line emission from plasma under the femtosecond pulse can be significantly enhanced.[5] Also, it has been experimentally demonstrated that by using temporally shaped pulse trains, the quality of femtosecond laser microstructuring of dielectrics[6,7] and silicon[8,9] can be improved. Although some explanations were given for possible reasons leading to better ablation quality, there is no theoretical analysis to directly support the results.

This study employs the plasma model recently developed by the authors[10–12] to investigate the pulse train ablation of dielectrics, in which quantum theories are employed to calculate the time and space dependent optical and thermal properties, including the electron heat capacity, electron relaxation time, electron conductivity, reflectivity, and absorption coefficient. It is shown that there exist constant ablation-depth zones with respect to fluences in the pulse train technology by which repeatable nanostructures can be obtained, even when the laser system is subject to some fluctuation in fluences. The details of the plasma model are explained in Refs. 11 and 12, and only several key equations are included in this paper. The following equation is used to calculate the free electron generation,[13] in which the electron decay term is also considered:[14]

$$\frac{\partial n_e(t,r,z)}{\partial t} = a_i I(t,r,z) n_e(t,r,z) + \delta_N (I(t,r,z))^N - \frac{n_e(t,r,z)}{\tau}, \tag{1}$$

where t is the time; r is the distance to the Gaussian beam axis; z is the depth from the surface of the bulk material; τ is the decay time constant; $n_e(t,r,z)$ is the free electron density; a_i is the impact ionization constant; $I(t,r,z)$ is the laser intensity inside the bulk material; and δ_N is the cross section of N-photon absorption. Based on experimental measurements of the threshold fluences, at the wavelength of 780 nm for fused silica, $a_i = 4 \pm 0.6\ \mathrm{cm}^2/\mathrm{J}$, $\delta_6 = 6 \times 10^{8\pm0.9}\ \mathrm{cm}^{-3}\ \mathrm{ps}^{-1}(\mathrm{cm}^2/\mathrm{TW})^6$,[15] and $\tau = 60$ fs.[14]

The original laser beam before it interacts with the material is assumed to be a Gaussian distribution in time and space. It is assumed that the laser focus point is at the material surface, $z=0$. Considering time and space dependent optical properties, the laser intensities inside the bulk materials are expressed as

$$I(t,r,z) = \frac{2F}{\sqrt{\pi/\ln 2}\, t_p}(1 - R(t,r)) \times \exp\left(-\frac{r^2}{r_0^2} - (4 \ln 2)\left(\frac{t}{t_p}\right)^2 - \int_0^z \alpha(t,r,z)dz \right), \tag{2}$$

where F is the laser fluence; t_p is the pulse duration; $R(t,r)$ is the reflectivity; r_0 is the radius of the laser beam; and $\alpha(t,r,z)$ is the absorption coefficient. The Drude model is used to determine the optical properties of the ionized dielectrics. The spatial and temporal dependent dielectric function of the plasma is expressed as

$$\epsilon(t,r,z) = 1 + \left(\frac{n_e(t,r,z)e^2}{m_e \epsilon_0}\right)\left(\frac{-\tau_e^2(t,r,z) + i\tau_e(t,r,z)/\omega}{1 + \omega^2 \tau_e^2(t,r,z)}\right), \tag{3}$$

where e is the electron charge; m_e is the mass of electron; ϵ_0 is the electrical permittivity of free space; $\tau_e(t,r,z)$ is the free electron relaxation time; and ω is the laser frequency. Based on Eq. (3), the absorption coefficient through free electron heating, $\alpha_h(t,r,z)$, and the reflectivity on the surface of the highly ionized dielectric, $R(t,r)$, can be determined by the Fresnel expression. The total absorption coefficient, α, accounting for both the free electron heating absorption and the absorption through avalanche ionization and multiphoton ionization is[10]

$$\alpha(t,r,z) = (a_i n_e(t,r,z) + \delta_N (I(t,r,z))^{N-1}) \times (\langle \varepsilon(t,r,z) \rangle + U_I), \tag{4}$$

where $\langle \varepsilon(t,r,z) \rangle$ is the average kinetic energy of free electrons and U_I is the band gap of materials. For fused silica, $U_I = 9$ eV.

[a)]Author to whom correspondence should be addressed; electronic mail: tsai@umr.edu.

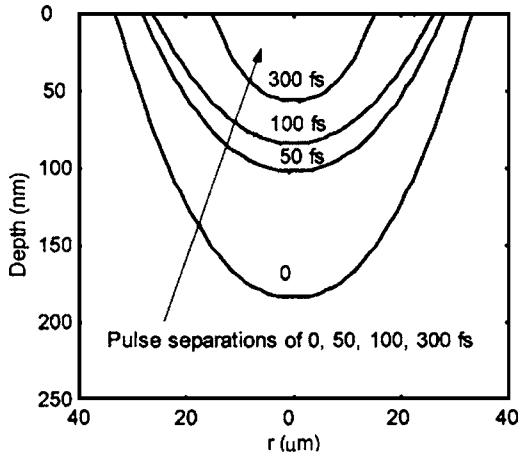

FIG. 1. Ablation crater shapes by pulse trains consisting of two pulses with the total fluence of 5 J/cm^2.

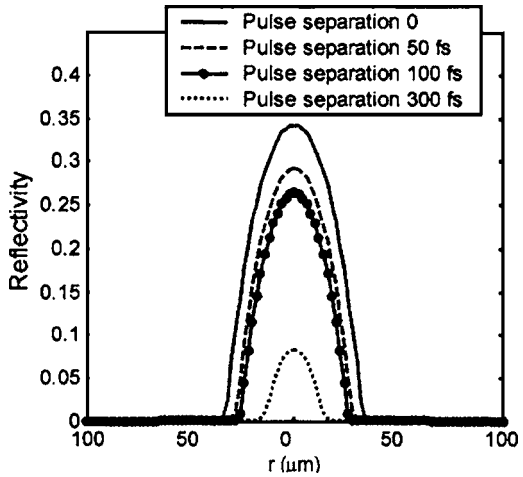

FIG. 2. Integrated reflectivity at $r=0$ and different pulse separation times for 2 pulses per train.

The free electron relaxation time in Eq. (3) is calculated by the following quantum estimation derived from the Boltzmann transportation equation:

$$\tau_e(t,r,z) = \frac{3\sqrt{m_e}(k_B T(t,r,z))^{3/2}}{2\sqrt{2}\pi(Z^*)^2 n_e(t,r,z)e^4 \ln\Lambda} \times (1+\exp(-\mu(n_e,T)/k_B T(t,r,z)))F_{1/2}, \quad (5)$$

where Z^* is the ionization state, k_B is the Boltzmann constant, T is the electron temperature, $F_{1/2}$ is the Fermi-Dirac integrals, μ is the chemical potential, and $\ln\Lambda$ is the Coulomb logarithm determined by $\ln\Lambda=0.5\ln(1+(b_{\max}/b_{\min})^2)$. $b_{\max}$ is the maximum collision parameter determined by $b_{\max}=(k_B T/m_e)^{1/2}/\max(\omega,\omega_p)$; where ω is the laser frequency and ω_p is the plasma frequency; $b_{\min}$ is the minimum collision parameter calculated by $b_{\min}=\max(Ze^2/k_B T, h/2\pi(m_e k_B T)^{1/2})$ where h is the Planck constant. For free electrons modeled as "particle in a box," the chemical potential can be calculated by

$$\mu(n_e,T) = \varepsilon_F(n_e) \times \left[1 - \frac{\pi^2}{12}\left(\frac{k_B T(t,r,z)}{\varepsilon_F(n_e)}\right)^2 + \frac{\pi^2}{80}\left(\frac{k_B T(t,r,z)}{\varepsilon_F(n_e)}\right)^4\right], \quad (6)$$

where ε_F is the Fermi energy that is determined by $\varepsilon_F(n_e)=((hc)^2/8m_e c^2)(3/\pi)^{2/3}(n_e(t,r,z))^{2/3}$ in which c is the scalar speed of light in vacuum. And the electron temperatures are determined by

$$c_e(T,n_e)n_e(t,r,z)\frac{\partial T(t,r,z)}{\partial t} = \alpha_h(t,r,z)I(t,r,z), \quad (7)$$

where c_e is the specific heat of free electrons, $c_e(T,n_e)=(\partial\langle E\rangle/\partial T)_V=(\partial\langle\varepsilon\rangle/\partial T)_V$. The average kinetic energy, $\langle\varepsilon\rangle$, is determined by the Fermi-Dirac distribution

$$\langle\varepsilon\rangle = \frac{\Sigma_k\langle n_k\rangle\varepsilon_k}{N_e} = \frac{\int_0^\infty \frac{1}{e^{\beta(T)(\varepsilon-\mu(n_e,T))}+1}\rho(\varepsilon)\varepsilon d\varepsilon}{\int_0^\infty \frac{1}{e^{\beta(T)(\varepsilon-\mu(n_e,T))}+1}\rho(\varepsilon)d\varepsilon}, \quad (8)$$

where $\beta(T)=1/k_B T(t,r,z)$ and $\rho(\varepsilon)=8\sqrt{2\varepsilon}\pi m_e^{3/2}/h^3$ is the density of states.

It is assumed that a small volume of dielectric material is ablated if its free electron density is equal to or above the critical electron density. For femtosecond lasers, the critical density, n_{cr}, is selected as the free electron density at which the plasma oscillation frequency is equal to the laser frequency. Thus, according to Eq. (3), $n_{cr}=4\pi^2 c^2 m_e\varepsilon_0/\lambda^2 e^2$, where λ is the wavelength of the laser.

This study calculates a 50 fs(t_p), 780 nm(λ) laser ablation of fused silica using a single pulse or pulse train. It is noted that the pulses within a train have the same fluence in our simulations. For a train consisting of one pulse, the ablation threshold fluence is found to be 3.3 J/cm^2. For 2 pulses per train, the ablation threshold is 1.8, 1.9, and 2.3 J/cm^2 per pulse, i.e., 3.6, 3.8, and 4.6 J/cm^2 per train, at the pulse separations of 50 fs, 100 fs, and 300 fs, respectively.

The ablation crater shapes are demonstrated in Fig. 1, in which the single pulse at 5 J/cm^2 is also considered as a train consisting of two pulses at 2.5 J/cm^2 each with zero pulse separation. At 5 J/cm^2 and the beam spot size of 100 μm, by using the train consisting of two pulses, the ablation depths are 184, 102, 84, and 56 nm, at the pulse separations of 0, 50, 100, and 300 fs, respectively. The corresponding ablation crater diameters are 66, 56, 52, and 30 μm, respectively, at the laser beam spot size of 100 μm.

The previous pulse has significant effects on the optical properties for the subsequent pulse within the same train. As shown in Fig. 2, the overall reflectivity integrated for the time period during the pulse irritation significantly decreases as the pulse separation increases. The highest overall reflectivities are 0.34, 0.29, 0.26, and 0.08 at the pulse separations of 0, 50, 100, and 300 fs, respectively.

Another important factor is the effect of fluence on the ablation depth as shown in Fig. 3. For comparison purpose, the fluences given in Fig. 3 are in terms of total fluence per train instead of per pulse. As shown in Fig. 3, there are constant ablation-depth zones with respect to fluences, which are due to the overall reflectivity and absorption coefficient significantly increasing with the increase of fluences.[10,11] If there exists a constant ablation-depth zone with respect to fluence, in similar conditions, a flat bottom crater would be formed under a Gaussian beam,[10,11] which has been experimentally observed.[16,17] Also, a constant ablation-depth zone

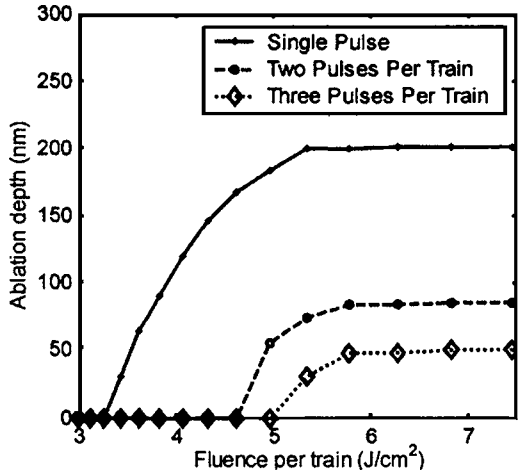

FIG. 3. The ablation depth as a function of fluence per train in which the fluence is in terms of total fluence per train instead of per pulse.

with respect to fluence has been directly demonstrated in experiments.[18]

What does a constant ablation-depth zone with respect to fluence mean in nano-/microfabrications? Because the laser pulse fluence may be subject to significant fluctuations in practice and the ablation depth is very sensitive to fluence variations at fluences slightly above the ablation threshold, it is rather difficult to control the accuracy for ablation depth at nanometer scales for the case of single pulse per train. For example, by a single pulse per train the ablation depth at 4 ± 0.5 J/cm^2 would vary in the range of 47–157 nm. Hence, a slight variation in fluence will result in a large difference in ablation depth. This explains the poor repeatability in the femtosecond ablation of nanostructures using fluences slightly above the ablation threshold. On the other hand, by using the single pulse, the ablation depth at 6.5 ± 0.5 J/cm^2 is quite stable and is around 200 nm, which is the theoretical limit of repeatable accuracy by the femtosecond single pulse per train in this case. In contrast, using two pulses per train with the pulse separation time of 300 fs, the ablation depth can be accurately controlled at around 85 nm at 6.5 ± 0.5 J/cm^2, which provides a potential method to achieve repeatable nanostructures with improved accuracy. In other words, by using the constant ablation-depth zones with respect to fluences, repeatable nanostructures can be obtained, even when the laser system is subject to the fluctuation in fluences. Also, through changing the pulse train parameters, it is possible to obtain desired repeatable ablation depths. For example, using 3 pulses per train with the pulse separation time of 200 fs, the ablation depth can be controlled around 49 nm at 6.5 ± 0.5 J/cm^2. In contrast, the constant ablation-depth zone is not changeable for the single pulse per train with the given wavelength and pulse duration.

In conclusion, the following major observations can be made from the calculations for fused silica: (1) at the same total fluence, the overall reflectivity significantly decreases as the pulse separation increases; (2) the pulse train technology can obtain smaller structures; (3) there exists constant ablation-depth zones with respect to fluences in femtosecond laser ablation of dielectrics; and (4) using pulse train technology repeatable nanostructures can be obtained, even when the laser system is subject to the fluctuation in laser fluences.

This work was supported by the National Science Foundation under Grant No. 0423233.

[1] R. Bartels, S. Backus, E. Zeek, L. Misoguti, G. Vdovin, I. P. Christov, M. M. Murnane, and H. C. Kapteyn, Nature (London) **406**, 164 (2000).
[2] A. Lindinger, C. Lupulescu, M. Plewicki, F. Vetter, A. Merli, M. S. Weber, and L. Wöste, Phys. Rev. Lett. **93**, 033001 (2004).
[3] M. Renard, E. Hertz, B. Lavorel, and O. Faucher, Phys. Rev. A **69**, 043401 (2004).
[4] A. Assion, T. Baumert, M. Bergt, T. Brixner, B. Kiefer, V. V. Seyfried, M. Strehle, and G. Gerber, Science **282**, 919 (1998).
[5] A. A. Andreev, J. Limpouch, A. B. Iskakov, and H. Nakano, Phys. Rev. E **65**, 026403 (2002).
[6] R. Stoian, A. Mermillod-Blondin, S. Winkler, A. Rosenfeld, I. V. Hertel, M. Spyridaki, E. Koudoumas, C. Fotakis, I. M. Burakov, and N. M. Bulgakova, Proc. SPIE Int. Opt. Eng. **5662**, 593 (2004).
[7] R. Stoian, M. Boyle, A. Thoss, A. Rosenfeld, G. Korn, I. V. Hertel, and E. E. B. Campbell, Appl. Phys. Lett. **80**, 353 (2002).
[8] M. Spyridaki, E. Koudoumas, P. Tzanetakis, C. Fotakis, R. Stoian, A. Rosenfeld, and I. V. Hertel, Appl. Phys. Lett. **83**, 1474 (2003).
[9] T. Y. Choi, D. J. Hwang, and C. P. Grigoropoulos, Appl. Surf. Sci. **197–198**, 720 (2002).
[10] L. Jiang and H. L. Tsai, J. Phys. D **37**, 1492 (2004).
[11] L. Jiang and H. L. Tsai, Int. J. Heat Mass Transfer **48**, 461 (2005).
[12] L. Jiang and H. L. Tsai, ASME J. Heat Transfer (in press).
[13] B. C. Stuart, M. D. Feit, A. M. Rubenchik, B. W. Shore, and M. D. Perry, Phys. Rev. Lett. **74**, 2248 (1995).
[14] M. Li, S. Menon, J. P. Nibarger, and G. N. Gibson, Phys. Rev. Lett. **82**, 2394 (1999).
[15] M. Lenzner, J. Krüger, S. Sartania, Z. Cheng, C. Spielmann, G. Mourou, W. Kautek, and F. Krausz, Phys. Rev. Lett. **80**, 4076 (1998).
[16] Z. Wu, H. Jiang, Z. Zhang, Q. Sun, H. Yang, and Q. Gong, Opt. Express **10**, 1244 (2002).
[17] J. Bonse, M. Munz, and H. Sturm, IEEE Nanotechnology **3**, 358 (2004).
[18] S. Nakamura, M. Hoshino, and Y. Ito, in Proceedings of ICALEO, October 2001, Jacksonville, FL, 2001.